IEEE Access
Multidisciplinary ⋮ Rapid Review ⋮ Open Access Journal

Received 7 June 2023, accepted 4 August 2023, date of publication 17 August 2023, date of current version 25 August 2023.

Digital Object Identifier 10.1109/ACCESS.2023.3305961

RESEARCH ARTICLE

A Closed-Form Solution for 3D Source Localization Using Angles and Doppler Shifted Frequencies

ZHU JIANDONG, DING TING, AND QIAO LIJUAN
Henan Province Engineering Research Center of High-speed Railway Operation and Maintenance, Zhengzhou 450000, China

Corresponding author: Zhu Jiandong (zhujiandong_zz@outlook.com)

This work was supported in part by the National Natural Science Foundation of China under Grant 62071490, in part by the Natural Science Foundation of Henan Province under Grant 222300420379, and in part by the Henan Province Higher Education Key Research Project under Grant 23B510016.

ABSTRACT Moving source localization in 3-D space using frequencies of arrival (FOA) have recently made significant progress with the development of closed-form solutions. However, the closed-form solution algorithms for source localization using FOA only introduces a large number of auxiliary variables and results in a significant jump in the minimum number of receivers. In order to overcome the inherent defect of source localization using FOA measurements only, we address locating the moving source by jointly using AOA and FOA measurements in this article. A closed-form solution is designed for AOA-FOA based source localization, where the AOA and FOA measurement noises, the carry frequency error, as well as the receiver location uncertainties are considered, and the two-stage weighted least squares (TSWLS) technique is applied to overcome the nonlinear relation between the measurements and the source location parameters. The proposed solution can give the source position and velocity estimate with much fewer receivers and nuisance parameters, and lower computational complexity, in comparison with the state-of-the-art FOA localization algorithm. The proposed solution is shown analytically and numerically to achieve the Cramer-Rao lower bound (CRLB) performance under small Gaussian noise conditions and outperform the FOA-only localization algorithm in terms of both CRLB and root mean square error under the same noise conditions.

INDEX TERMS Source localization, closed-form solution, frequency of arrival, angle of arrival, two-stage weighted least squares.

I. INTRODUCTION

As is well-known that source localization techniques have been widely used in fields such as wireless communication, navigation, source monitoring, air traffic control, security management, and many others [1], [2], [3], [4], which are important for both industrial production and national defense security.

Generally speaking, source localization can be performed based on different types of measurements of its emitted signal observed by spatially separated receivers, including time, frequency, angle, etc. For a stationary emitter, one common technique is to measure the time information of the source signal arriving at the receivers. The time measurements, such as time of arrival (TOA) [5], [6], [7] or time difference of arrival (TDOA) [8], [9], [10], [11] define, respectively, a set of circles or hyperbolas on which the source is located. By intersection of the curves associated with the time measurements of all receivers, an estimate of the source location parameters can be obtained. When the source is moving, frequency measurements such as frequency of arrival (FOA) [12], [13], [14], [15], [16], [17], [18] or frequency difference of arrival (FDOA) [19], [20], [21], can also be used to estimate accurately the source position and velocity. Source localization can also be applied based on angle of arrival (AOA) measurements [22], [23], [24] to enhance

The associate editor coordinating the review of this manuscript and approving it for publication was Mohammad Zia Ur Rahman.

localization accuracy. Each type of these measurements has its own applicable localization scenarios.

However, under certain conditions or practical constraints, it can be difficult, expensive, unreliable, or even impossible to acquire another type of measurements other than AOA and FOA. For instance, the time measurements can be extremely inaccurate for some narrowband or long pulse signals [19]. In addition, TOA measurements require time stamping of the emitted signal and all receivers within the network has to be accurately synchronized [25]. When utilizing TDOA or FDOA measurements, timestamp information is not required, but the receivers must be kept synchronized [26]. By contrast, FOA measurements have a relatively lower requirement on transmit-receive devices, can be implemented at a much lower cost, and have good measurement accuracy for some narrowband signals [12], [19]. These facts therefore motivate the academic research on FOA only localization issues, and some effective localization algorithms have been available from the literature [17], [18]. However, these FOA only localization algorithms need to introduce a fair number of auxiliary parameters and hence require more receivers to yield sufficient number of measurement equations, which limits its application in practice. To overcome this difficulty, a few suggestions have been put forward, one of which is employing a joint localization scheme based on the AOA and FOA measurements.

In this article we shall consider the scenario of localizing a moving source in the three-dimensional space using an array of moving receivers by the AOA and FOA measurements. Nonetheless, the source location parameters are associated in a nonlinear fashion with the AOA and FOA measurements, which makes the exploitation of AOA and FOA measurements challenging. Some efforts have been devoted to handle this challenging problem. These studies mainly focus on tracking the location of a moving source using AOA and FOA measurements [27], [28], [29], [30]. Such tracking algorithms, however, require AOA and FOA measurements observed at multiple time instants, and a good initial estimate near the true value of source location is often needed to start tracking, which is not always easy to obtain in practice. Not only that, but these tracking algorithms have no optimality properties, and their performance depends on the accuracy of the linearization in the measurement equation.

Determining the source position and velocity from AOA and FOA measurements obtained at a single time instant is not a trivial task. This is due to the highly nonlinear relation between the source location parameters and the AOA and FOA measurements. There are two research ideas to this problem, including the iterative Taylor-series method and the closed-form solution method. The closed-form solution is more appealing since it is free from initial value dependence and divergence problems and has good robustness and low computational complexity. However, for the AOA-FOA based source localization problem, to our knowledge, there is no corresponding closed-form solution in the open literature.

Motivated by these facts, we will present in this paper a computationally attractive closed-form solution for the AOA-FOA based source localization problem. This study borrows the basic idea of the well-known two-stage weighted least squares (TSWLS) by Ho and Xu [31], but is innovative for the AOA-FOA based source localization problem. By employing a joint localization scheme based on the AOA and FOA measurements, the proposed solution gives the source position and velocity estimate with much fewer receivers and auxiliary parameters in comparison with the state-of-the-art FOA-only localization method. Due to the application of TSWLS framework in the proposed solution, there is no initial value dependence and divergence problem, as in iterative method. Theoretical analysis and numerical simulations are performed, validating the proposed solution reaches the CRLB under small Gaussian noise conditions and attains better performance than the previous algorithms.

The rest of the paper is organized as follows. Section II formulates the localization problem mathematically. Section III presents the proposed solution. Section IV includes analytical study of the proposed solution. Section V evaluates the localization accuracy of the proposed solution by comparing with existing algorithms as well as the CRLB. Finally, conclusions are drawn in Section VI.

II. PROBLEM FORMULATION

Consider a three-dimensional space with an array of M receivers deployed to locate a moving source. The position and velocity of the receivers are known as $\mathbf{s}_m^{\mathrm{o}} = [x_m^{\mathrm{o}}, y_m^{\mathrm{o}}, z_m^{\mathrm{o}}]^T$ and $\dot{\mathbf{s}}_m^{\mathrm{o}} = [\dot{x}_m^{\mathrm{o}}, \dot{y}_m^{\mathrm{o}}, \dot{z}_m^{\mathrm{o}}]^T$ for $m = 1, 2, \ldots, M$. The position and velocity of the moving source to be located are noted as $u^{\mathrm{o}} = [x^{\mathrm{o}}, y^{\mathrm{o}}, z^{\mathrm{o}}]^T$ and $\dot{u}^{\mathrm{o}} = [\dot{x}^{\mathrm{o}}, \dot{y}^{\mathrm{o}}, \dot{z}^{\mathrm{o}}]^T$, respectively. The receivers intercept the signal from the source, and then estimate the source position and velocity by using AOA and FOA measurements of the signal.

According to the geometric relationship between the source and the receiver, the AOA pair corresponding to the mth receiver, which consists of the azimuth angle θ_m^{o} and the elevation angle φ_m^{o}, can be given by

$$\theta_m^{\mathrm{o}} = \arctan\left(\frac{y^{\mathrm{o}} - y_m^{\mathrm{o}}}{x^{\mathrm{o}} - x_m^{\mathrm{o}}}\right) \tag{1}$$

$$\varphi_m^{\mathrm{o}} = \arctan\left[\frac{z^{\mathrm{o}} - z_m^{\mathrm{o}}}{(x^{\mathrm{o}} - x_m^{\mathrm{o}})\cos\theta_m^{\mathrm{o}} + (y^{\mathrm{o}} - y_m^{\mathrm{o}})\cos\theta_m^{\mathrm{o}}}\right] \tag{2}$$

The azimuth angle and elevation angle measurements are inevitably corrupted by random noises such that the faulty values are

$$\theta_m = \theta_m^{\mathrm{o}} + \Delta\theta_m \tag{3}$$

$$\varphi_m = \varphi_m^{\mathrm{o}} + \Delta\varphi_m \tag{4}$$

where $\Delta\theta_m$ and $\Delta\varphi_m$ are the measurement noises of azimuth angle and elevation angle, respectively.

Due to the relative motion between the receiver and the source, the ideal Doppler shifted frequency observed by the

mth receiver is related to the source position and velocity by

$$f_m^{\mathrm{o}} = f_{\mathrm{c}}^{\mathrm{o}} - \frac{f_{\mathrm{c}}^{\mathrm{o}}}{c}\frac{(\mathbf{u}^{\mathrm{o}} - \mathbf{s}_m^{\mathrm{o}})^{\mathrm{T}}(\dot{\mathbf{u}}^{\mathrm{o}} - \dot{\mathbf{s}}_m^{\mathrm{o}})}{\| \mathbf{u}^{\mathrm{o}} - \mathbf{s}_m^{\mathrm{o}} \|} \tag{5}$$

where c is the known and constant signal propagation speed, $f_{\mathrm{c}}^{\mathrm{o}}$ is the signal carrier frequency. Correspondingly, the actual observed FOA measurement for the mth receiver can be written as

$$f_m = f_m^{\mathrm{o}} + \Delta f_m \tag{6}$$

where Δf_m is the FOA measurement noise.

By defining the following notations:

$$\begin{aligned}
\boldsymbol{\theta} &= [\theta_1, \theta_2, \ldots, \theta_M]^{\mathrm{T}}, \\
\boldsymbol{\varphi} &= [\varphi_1, \varphi_2, \ldots, \varphi_M]^{\mathrm{T}}, \\
\mathbf{f} &= [f_1, f_2, \ldots, f_M]^{\mathrm{T}}
\end{aligned} \tag{7}$$

$$\begin{aligned}
\boldsymbol{\theta}^{\mathrm{o}} &= [\theta_1^{\mathrm{o}}, \theta_2^{\mathrm{o}}, \ldots, \theta_M^{\mathrm{o}}]^{\mathrm{T}}, \\
\boldsymbol{\varphi}^{\mathrm{o}} &= [\varphi_1^{\mathrm{o}}, \varphi_2^{\mathrm{o}}, \ldots, \varphi_M^{\mathrm{o}}]^{\mathrm{T}}, \\
\mathbf{f}^{\mathrm{o}} &= [f_1^{\mathrm{o}}, f_2^{\mathrm{o}}, \ldots, f_M^{\mathrm{o}}]^{\mathrm{T}}
\end{aligned} \tag{8}$$

$$\begin{aligned}
\Delta\boldsymbol{\theta} &= [\Delta\theta_1, \Delta\theta_2, \ldots, \Delta\theta_M]^{\mathrm{T}}, \\
\Delta\boldsymbol{\varphi} &= [\Delta\varphi_1, \Delta\varphi_2, \ldots, \Delta\varphi_M]^{\mathrm{T}}, \\
\Delta\mathbf{f} &= [\Delta f_1, \Delta f_2, \ldots, \Delta f_M]^{\mathrm{T}}
\end{aligned} \tag{9}$$

we can put the AOA and FOA measurements into vector for easier manipulation as

$$\mathbf{m} = \mathbf{m}^{\mathrm{o}} + \Delta\mathbf{m} \tag{10}$$

where $\mathbf{m}^{\mathrm{o}} = [(\theta^{\mathrm{o}})^{\mathrm{T}}, (\varphi^{\mathrm{o}})^{\mathrm{T}}, (f^{\mathrm{o}})^{\mathrm{T}}]^{\mathrm{T}}$ is the noise-free AOA-FOA vector, $\mathbf{m} = [\theta^{\mathrm{T}}, \varphi^{\mathrm{T}}, f^{\mathrm{T}}]^{\mathrm{T}}$ is the erroneous AOA-FOA measurement vector, $\Delta\mathbf{m} = [\Delta\theta^{\mathrm{T}}, \Delta\varphi^{\mathrm{T}}, \Delta f^{\mathrm{T}}]^{\mathrm{T}}$ is the associated AOA-FOA measurement noise vector assumed to be zero-mean Gaussian with covariance matrix $\mathbf{Q}_{\mathbf{m}}$.

Actually, the exact positions and velocities of the receivers are not known, and we have only access to the erroneous version as

$$\mathbf{s}_m = \mathbf{s}_m^{\mathrm{o}} + \Delta\mathbf{s}_m \tag{11}$$

$$\dot{\mathbf{s}}_m = \dot{\mathbf{s}}_m^{\mathrm{o}} + \Delta\dot{\mathbf{s}}_m \tag{12}$$

where $\Delta\mathbf{s}_m$ and $\Delta\dot{\mathbf{s}}_m$ are the position and velocity error of the mth receiver.

By defining the following notations:

$$\mathbf{s} = [\mathbf{s}_1^T, \mathbf{s}_2^T, \ldots, \mathbf{s}_M^T]^T, \ \dot{\mathbf{s}} = [\dot{\mathbf{s}}_1^T, \dot{\mathbf{s}}_2^T, \ldots, \dot{\mathbf{s}}_M^T]^T \tag{13}$$

$$\mathbf{s}^{\mathrm{o}} = [(\mathbf{s}_1^{\mathrm{o}})^T, \ldots, (\mathbf{s}_M^{\mathrm{o}})^T]^T, \ \dot{\mathbf{s}}^{\mathrm{o}} = [(\dot{\mathbf{s}}_1^{\mathrm{o}})^T, \ldots, (\dot{\mathbf{s}}_M^{\mathrm{o}})^T]^T \tag{14}$$

$$\Delta\mathbf{s} = [\Delta\mathbf{s}_1^T, \Delta\mathbf{s}_2^T, \ldots, \Delta\mathbf{s}_M^T]^T,$$

$$\Delta\dot{\mathbf{s}} = [\Delta\dot{\mathbf{s}}_1^T, \Delta\dot{\mathbf{s}}_2^T, \ldots, \Delta\dot{\mathbf{s}}_N^T]^T \tag{15}$$

$$\mathbf{r} = [\mathbf{s}^{\mathrm{T}}, \dot{\mathbf{s}}^{\mathrm{T}}]^{\mathrm{T}} \tag{16}$$

$$\mathbf{r}^{\mathrm{o}} = [(\mathbf{s}^{\mathrm{o}})^{\mathrm{T}}, (\dot{\mathbf{s}}^{\mathrm{o}})^{\mathrm{T}}]^{\mathrm{T}} \tag{17}$$

$$\Delta\mathbf{r} = [\Delta\mathbf{s}^{\mathrm{T}}, \Delta\dot{\mathbf{s}}^{\mathrm{T}}]^{\mathrm{T}} \tag{18}$$

we can write the faulty positions and velocities of the receivers in vector form as

$$\mathbf{r} = \mathbf{r}^{\mathrm{o}} + \Delta\mathbf{r} \tag{19}$$

where $\mathbf{r}^{\mathrm{o}} = [(\mathbf{s}^{\mathrm{o}})^{\mathrm{T}}, (\dot{\mathbf{s}}^{\mathrm{o}})^{\mathrm{T}}]^{\mathrm{T}}$ is the true receiver position-velocity vector, $\mathbf{r} = [\mathbf{s}^{\mathrm{T}}, \dot{\mathbf{s}}^{\mathrm{T}}]^{\mathrm{T}}$ is the erroneous receiver position-velocity vector, $\Delta\mathbf{r} = [\Delta\mathbf{s}^{\mathrm{T}}, \Delta\dot{\mathbf{s}}^{\mathrm{T}}]^{\mathrm{T}}$ is the associated receiver position-velocity error vector assumed to be zero-mean Gaussian with covariance matrix $\mathbf{Q}_{\mathbf{r}}$.

The true value of the carrier frequency $f_{\mathrm{c}}^{\mathrm{o}}$ is also not known, especially in the non-cooperative case. Usually only a rough estimate with uncertainties gathered from the past is available as

$$f_{\mathrm{c}} = f_{\mathrm{c}}^{\mathrm{o}} + \Delta f_{\mathrm{c}} \tag{20}$$

where f_{c} is the erroneous version of the carrier frequency, Δf_{c} is the carrier frequency error assumed to be Gaussian with zero-mean and variance σ_{c}^2.

Using the AOA-FOA measurements $\mathbf{m}$, the erroneous receiver position-velocity $\mathbf{r}$ and carrier frequency f_{c}, we aim to estimate the unknown source position and velocity as accurately as possible. However, due to the nonconvexity of measurement equations with respect to the unknowns, the localization problem is not a trivial task.

III. CLOSED-FORM LOCALIZATION METHOD

In this section, we design a closed-form solution for estimating the source position and velocity, with the aim of attaining the CRLB performance. To overcome the nonconvexity of measurement equations, we convert the nonlinear the measurement equations to the pseudolinear ones by introducing proper auxiliary parameters. Subsequently, a closed-form solution is proposed based on the well-known TSWLS framework.

A. FIRST STAGE

We first handle the AOA measurements by taking the tangent from both sides of (1) and (2), and then cross-multiplying, which yields the azimuth angle and elevation angle equations in linear form as:

$$(\mathbf{a}_m^{\mathrm{o}})^T\mathbf{u}^{\mathrm{o}} = (\mathbf{a}_m^{\mathrm{o}})^T\mathbf{s}_m^{\mathrm{o}} \tag{21}$$

$$(\mathbf{b}_m^{\mathrm{o}})^T\mathbf{u}^{\mathrm{o}} = (\mathbf{b}_m^{\mathrm{o}})^T\mathbf{s}_m^{\mathrm{o}} \tag{22}$$

where

$$\mathbf{a}_m^{\mathrm{o}} = [\sin(\theta_m^{\mathrm{o}}), -\cos(\theta_m^{\mathrm{o}}), 0]^{\mathrm{T}} \tag{23}$$

$$\mathbf{b}_m^{\mathrm{o}} = [\sin(\varphi_m^{\mathrm{o}})\cos(\theta_m^{\mathrm{o}}), \sin(\varphi_m^{\mathrm{o}})\sin(\theta_m^{\mathrm{o}}), -\cos(\varphi_m^{\mathrm{o}})]^{\mathrm{T}} \tag{24}$$

Substituting the noisy AOA measurements and the erroneous receiver positions into (21) and (22), and then using the first order Taylor series expansion, we have

$$\boldsymbol{\rho}_{\mathrm{a},m}^T(\mathbf{s}_m - \mathbf{u}^{\mathrm{o}})\Delta\theta_m + \mathbf{a}_m^T\Delta\mathbf{s}_m = \mathbf{a}_m^T\mathbf{s}_m - \mathbf{a}_m^T\mathbf{u}^{\mathrm{o}} \tag{25}$$

$$\boldsymbol{\rho}_{\mathrm{b},\theta,m}^T(\mathbf{s}_m - \mathbf{u}^{\mathrm{o}})\Delta\theta_m + \boldsymbol{\rho}_{\mathrm{b},\varphi,m}^T(\mathbf{s}_m - \mathbf{u}^{\mathrm{o}})\Delta\varphi_m + \mathbf{b}_m^T\Delta\mathbf{s}_m = \mathbf{b}_m^T\mathbf{s}_m - \mathbf{b}_m^T\mathbf{u}^{\mathrm{o}} \tag{26}$$

where

$$\boldsymbol{\rho}_{\mathrm{a},m} = [\cos(\theta_m), \sin(\theta_m), 0]^{\mathrm{T}} \tag{27}$$

$$\boldsymbol{\rho}_{\mathrm{b},\theta,m}^{T} = [-\sin(\varphi_m)\sin(\theta_m), \sin(\varphi_m)\cos(\theta_m), 0]^{\mathrm{T}} \tag{28}$$

$$\boldsymbol{\rho}_{\mathrm{b},\varphi,m}^{T} = [\cos(\varphi_m)\cos(\theta_m), \cos(\varphi_m)\sin(\theta_m), \sin(\varphi_m)]^{\mathrm{T}} \tag{29}$$

Next, we handle the FOA measurements by jointly using AOA information. For ease of presentation, we first rewrite (5) as

$$r_m^{\mathrm{o}} = \frac{c(f_{\mathrm{c}}^{\mathrm{o}} - f_m^{\mathrm{o}})}{f_{\mathrm{c}}^{\mathrm{o}}} = \frac{(\mathbf{u}^{\mathrm{o}} - \mathbf{s}_m^{\mathrm{o}})^{\mathrm{T}}(\dot{\mathbf{u}}^{\mathrm{o}} - \dot{\mathbf{s}}_m^{\mathrm{o}})}{\parallel \mathbf{u}^{\mathrm{o}} - \mathbf{s}_m^{\mathrm{o}} \parallel} \tag{30}$$

Multiplying the denominator term on the right side of (30) with the left side, yields

$$(\mathbf{u}^{\mathrm{o}})^{\mathrm{T}}\dot{\mathbf{u}}^{\mathrm{o}} - (\dot{\mathbf{s}}_m^{\mathrm{o}})^{\mathrm{T}}\mathbf{u}^{\mathrm{o}} - (\mathbf{s}_m^{\mathrm{o}})^{\mathrm{T}}\dot{\mathbf{u}}^{\mathrm{o}} + (\mathbf{s}_m^{\mathrm{o}})^{\mathrm{T}}\dot{\mathbf{s}}_m^{\mathrm{o}} = r_m^{\mathrm{o}} \parallel \mathbf{u}^{\mathrm{o}} - \mathbf{s}_m^{\mathrm{o}} \parallel \tag{31}$$

Using the fact that

$$\parallel \mathbf{u}^{\mathrm{o}} - \mathbf{s}_m^{\mathrm{o}} \parallel = \frac{z^{\mathrm{o}} - z_m^{\mathrm{o}}}{\sin(\varphi_m^{\mathrm{o}})} \tag{32}$$

we can rearrange (31) as

$$(\mathbf{u}^{\mathrm{o}})^{\mathrm{T}}\dot{\mathbf{u}}^{\mathrm{o}} - (\dot{\mathbf{s}}_m^{\mathrm{o}})^{\mathrm{T}}\mathbf{u}^{\mathrm{o}} - (\mathbf{s}_m^{\mathrm{o}})^{\mathrm{T}}\dot{\mathbf{u}}^{\mathrm{o}} + (\mathbf{s}_m^{\mathrm{o}})^{\mathrm{T}}\dot{\mathbf{s}}_m^{\mathrm{o}} = \frac{(z^{\mathrm{o}} - z_m^{\mathrm{o}})r_m^{\mathrm{o}}}{\sin(\varphi_m^{\mathrm{o}})} \tag{33}$$

Similarly, substituting the noisy AOA-FOA measurements, the erroneous receiver position-velocity and carrier frequency into (33), and then using the first order Taylor series expansion, we have

$$\begin{aligned} &-(\mathbf{u}^{\mathrm{o}})^{\mathrm{T}}\Delta\dot{\mathbf{s}}_m + \frac{z^{\mathrm{o}}}{\sin(\varphi_m)}\frac{c}{f_{\mathrm{c}}}\Delta f_m - \frac{z^{\mathrm{o}}}{\sin(\varphi_m)}\frac{cf_m}{f_{\mathrm{c}}^2}\Delta f_{\mathrm{c}} \\ &-\frac{\cos(\varphi_m)r_m z^{\mathrm{o}}}{\sin(\varphi_m)^2}\Delta\varphi_m - (\dot{\mathbf{u}}^{\mathrm{o}})^{\mathrm{T}}\Delta\mathbf{s}_m + \frac{r_m}{\sin(\varphi_m)}\Delta z_m = \\ &\frac{r_m z_m}{\sin(\varphi_m)} + \mathbf{s}_m^{\mathrm{T}}\dot{\mathbf{s}}_m - \dot{\mathbf{s}}_m^{\mathrm{T}}\mathbf{u}^{\mathrm{o}} - \frac{r_m z^{\mathrm{o}}}{\sin(\varphi_m)} - \mathbf{s}_m^{\mathrm{T}}\dot{\mathbf{u}}^{\mathrm{o}} + (\mathbf{u}^{\mathrm{o}})^{\mathrm{T}}\dot{\mathbf{u}}^{\mathrm{o}} \end{aligned} \tag{34}$$

Note that (34) is nonlinear with respect to source position-velocity but appears to be linear with respect to the source position-velocity and the unknown $(\mathbf{u}^{\mathrm{o}})^{\mathrm{T}}\dot{\mathbf{u}}^{\mathrm{o}}$. The idea here is to introduce $(\mathbf{u}^{\mathrm{o}})^{\mathrm{T}}\dot{\mathbf{u}}^{\mathrm{o}}$ as the auxiliary parameter and define an auxiliary vector as follow

$$\boldsymbol{\eta}_1^{\mathrm{o}} = [(\mathbf{u}^{\mathrm{o}})^{\mathrm{T}}, (\dot{\mathbf{u}}^{\mathrm{o}})^{\mathrm{T}}, (\mathbf{u}^{\mathrm{o}})^{\mathrm{T}}\dot{\mathbf{u}}^{\mathrm{o}}]^{\mathrm{T}} \tag{35}$$

Stacking the pseudolinear equations in (25) and (26) for M receivers yields in matrix form

$$\Delta\mathbf{h}_1 = \mathbf{h}_1 - \mathbf{G}_1\boldsymbol{\eta}_1^{\mathrm{o}} \tag{36}$$

where

$$\begin{aligned} [\mathbf{G}_1]_{m,1:3} &= \mathbf{a}_m^T \\ [\mathbf{G}_1]_{M+m,1:3} &= \mathbf{b}_m^T \\ [\mathbf{G}_1]_{2M+m,1:3} &= \left[\dot{x}_m, \dot{y}_m, \dot{z}_m + \frac{r_m}{\sin(\varphi_m)}\right] \\ [\mathbf{G}_1]_{2M+m,4:6} &= \mathbf{s}_m^{\mathrm{T}} \\ [\mathbf{G}_1]_{2M+m,7} &= -1 \end{aligned} \tag{37}$$

$$\begin{aligned} [\mathbf{h}_1]_m &= \mathbf{a}_m^T\mathbf{s}_m \\ [\mathbf{h}_1]_{M+m} &= \mathbf{b}_m^T\mathbf{s}_m \\ [\mathbf{h}_1]_{2M+m} &= \frac{r_m z_m}{\sin(\varphi_m)} + \mathbf{s}_m^{\mathrm{T}}\dot{\mathbf{s}}_m \end{aligned} \tag{38}$$

where $\Delta\mathbf{h}_1$ is the error term related to the unknowns by

$$\Delta\mathbf{h}_1 = \mathbf{B}_1\Delta\boldsymbol{\alpha} + \mathbf{D}_1\Delta\boldsymbol{\beta} + \mathbf{c}_1\Delta f_{\mathrm{c}} \tag{39}$$

with

$$\begin{aligned} [\mathbf{B}_1]_{m,m} &= \boldsymbol{\rho}_{\mathrm{a},m}^T(\mathbf{s}_m^{\mathrm{o}} - \mathbf{u}^{\mathrm{o}}) \\ [\mathbf{B}_1]_{M+m,m} &= \boldsymbol{\rho}_{\mathrm{b},\theta,m}^T(\mathbf{s}_m - \mathbf{u}^{\mathrm{o}}) \\ [\mathbf{B}_1]_{M+m,M+m} &= \boldsymbol{\rho}_{\mathrm{b},\varphi,m}^T(\mathbf{s}_m - \mathbf{u}^{\mathrm{o}}) \\ [\mathbf{B}_1]_{2M+m,M+m} &= \frac{(z_m - z^{\mathrm{o}})\cos(\varphi_m)r_m}{\sin(\varphi_m)^2} \\ [\mathbf{B}_1]_{2M+m,2M+m} &= -\frac{z^{\mathrm{o}}c}{\sin(\varphi_m)f_{\mathrm{c}}} \end{aligned} \tag{40}$$

$$[\mathbf{c}_1]_{2M+m,1} = \frac{(\dot{z}_m - \dot{z}^{\mathrm{o}})}{\sin(\varphi_m)}\frac{cf_m}{f_{\mathrm{c}}^2} \tag{41}$$

$$\begin{aligned} [\mathbf{D}_1]_{m,3m-2:3m} &= \mathbf{a}_m^T \\ [\mathbf{D}_1]_{M+m,3m-2:3m} &= \mathbf{b}_m^T \\ [\mathbf{D}_1]_{2M+m,3m-2:3m} &= \left[\dot{x}_m - \dot{x}^{\mathrm{o}}, \dot{y}_m - \dot{y}^{\mathrm{o}}, \dot{z}_m - \dot{z}^{\mathrm{o}} + \frac{r_m}{\sin(\varphi_m)}\right] \\ [\mathbf{D}_1]_{2M+m,3M+3m-2:3M+3m} &= (\mathbf{s}_m - \mathbf{u}^{\mathrm{o}})^{\mathrm{T}} \end{aligned} \tag{42}$$

for $m = 1, 2, \ldots, M$ and zeros elsewhere. Assuming that $\Delta\mathbf{m}$, $\Delta\mathbf{r}$, and Δf_{c} are mutually independent, $\Delta\mathbf{h}_1$ can be considered as zero-mean Gaussian distributed with the covariance matrix equal to

$$\begin{aligned} \mathbf{Q} &= E(\Delta\mathbf{h}_1\Delta\mathbf{h}_1^T) \\ &= \mathbf{B}_1\mathbf{Q}_{\mathbf{m}}\mathbf{B}_1^T + \mathbf{D}_1\mathbf{Q}_{\mathbf{r}}\mathbf{D}_1^T + \sigma_{f\mathrm{c}}^2\mathbf{c}_f\mathbf{c}_f^T \\ &= \mathbf{B}_1\mathbf{Q}_{\mathbf{m}}\mathbf{B}_1^T + \mathbf{A}_1\mathbf{Q}_{\mathbf{n}}\mathbf{A}_1^T \end{aligned} \tag{43}$$

where $\mathbf{Q}_{\mathbf{n}} = blkdiag\{\sigma_{f\mathrm{c}}^2, \mathbf{Q}_{\mathbf{r}}\}$ and $\mathbf{a}_1 = [\mathbf{c}_f, \mathbf{D}_1]$. By minimizing the weighted error energy $\Delta\mathbf{h}_1^T\mathbf{W}_1\Delta\mathbf{h}_1$ with respect to η_1^{o}, we obtain the WLS estimate of $\boldsymbol{\eta}_1^{\mathrm{o}}$ as

$$\boldsymbol{\eta}_1 = (\mathbf{G}_1^T\mathbf{W}_1\mathbf{G}_1)^{-1}\mathbf{G}_1^T\mathbf{W}_1\mathbf{h}_1 \tag{44}$$

where $\mathbf{W}_1$ is the weighting matrix equal to

$$\begin{aligned} \mathbf{W}_1 &= \left[\mathrm{E}(\Delta\mathbf{h}_1\Delta\mathbf{h}_1^{\mathrm{T}})\right]^{-1} \\ &= \left[\mathbf{B}_1\mathbf{Q}_{\mathbf{m}}\mathbf{B}_1^T + \mathbf{A}_1\mathbf{Q}_{\mathbf{n}}\mathbf{A}_1^T\right]^{-1} \end{aligned} \tag{45}$$

Observe that $\mathbf{W}_1$ is related to the unknowns in $\boldsymbol{\eta}_1^{\mathrm{o}}$, and hence cannot be calculated straightforwardly. Instead, we implement the algorithm by updating $\mathbf{W}_1$ and $\boldsymbol{\eta}_1^{\mathrm{o}}$ iteratively. Specifically, we first initialize the weighting matrix as $\mathbf{W}_1 = \mathbf{I}$,

and then use (44) to yield an initial estimate $\boldsymbol{\eta}_1$. $\boldsymbol{\eta}_1$ is then substituted into (45) to update $\mathbf{W}_1$, which in turn is employed to produce a more accurate estimate $\boldsymbol{\eta}_1$.

Combining $\boldsymbol{\eta}_1^{\mathrm{o}} = (\mathbf{G}_1^T\mathbf{W}_1\mathbf{G}_1)^{-1}\mathbf{G}_1^T\mathbf{W}_1\mathbf{G}_1\boldsymbol{\eta}_1^{\mathrm{o}}$ and (44) leads to

$$\Delta\boldsymbol{\eta}_1 = \boldsymbol{\eta}_1 - \boldsymbol{\eta}_1^{\mathrm{o}} = (\mathbf{G}_1^T\mathbf{W}_1\mathbf{G}_1)^{-1}\mathbf{G}_1^T\mathbf{W}_1\Delta\mathbf{h}_1 \tag{46}$$

It can be deduced from (46) that $E(\Delta\boldsymbol{\eta}_1)$ approximates zero, which shows that $\boldsymbol{\eta}_1$ is approximately unbiased. The covariance matrix of $\boldsymbol{\eta}_1$ can be approximately as

$$cov(\boldsymbol{\eta}_1) = (\mathbf{G}_1^{\mathrm{T}}\mathbf{W}_1\mathbf{G}_1)^{-1} \tag{47}$$

B. SECOND STAGE

As can be seen from the first-stage estimate in (44), the introduced nuisance parameter $(\mathbf{u}^{\mathrm{o}})^{\mathrm{T}}\dot{\mathbf{u}}^{\mathrm{o}}$ in η_1^{o} is a function of source location parameters $\mathbf{u}^{\mathrm{o}}$ and $\dot{\mathbf{u}}^{\mathrm{o}}$. The function relationship between the auxiliary parameter and the source location parameters will be exploited in the second stage to refine the first-stage estimate. For this purpose, we define a vector as

$$\boldsymbol{\eta}_2^{\mathrm{o}} = [(\mathbf{u}^{\mathrm{o}})^{\mathrm{T}}, \mathbf{u}^{\mathrm{o}} \odot \dot{\mathbf{u}}^{\mathrm{o}}]^{\mathrm{T}} \tag{48}$$

where the symbol $\odot$ represents element by element multiplication. Ignoring the second-order error terms, we can express the source location parameters in $\boldsymbol{\eta}_2^{\mathrm{o}}$ with respect to the first-stage estimate $\boldsymbol{\eta}_1$ as

$$\mathbf{u}^{\mathrm{o}} = \boldsymbol{\eta}_1(1:3) - \Delta\eta_1(1:3) \tag{49}$$

$$\mathbf{u}^{\mathrm{o}} \odot \dot{\mathbf{u}}^{\mathrm{o}} = \boldsymbol{\eta}_1(1:3) \odot \boldsymbol{\eta}_1(4:6) - 2\boldsymbol{\eta}_1(1:3) \odot \Delta\boldsymbol{\eta}_1(4:6) - 2\boldsymbol{\eta}_1(4:6) \odot \Delta\boldsymbol{\eta}_1(1:3) \tag{50}$$

$$(\mathbf{u}^{\mathrm{o}})^{\mathrm{T}}(\dot{\mathbf{u}}^{\mathrm{o}}) = \boldsymbol{\eta}_1(1:3)^{\mathrm{T}}\boldsymbol{\eta}_1(4:6) - \Delta\boldsymbol{\eta}_1(7) \tag{51}$$

Collecting the equations (49)-(51) gives, in matrix form

$$\Delta\mathbf{h}_2 = \mathbf{h}_2 - \mathbf{G}_2\boldsymbol{\eta}_2^{\mathrm{o}} \tag{52}$$

where

$$\begin{aligned} [\mathbf{G}_2]_{1:3,1:3} &= \mathbf{I} \\ [\mathbf{G}_2]_{4:6,4:6} &= \mathbf{I} \\ [\mathbf{G}_1]_{7,4:6} &= 1^{\mathrm{T}} \end{aligned} \tag{53}$$

$$\begin{aligned} [\mathbf{h}_2]_{1:3} &= \boldsymbol{\eta}_1(1:3) \\ [\mathbf{h}_2]_{4:6} &= \boldsymbol{\eta}_1(1:3) \odot \boldsymbol{\eta}_1(4:6) \\ [\mathbf{h}_2]_7 &= \boldsymbol{\eta}_1(7) \end{aligned} \tag{54}$$

The error vector $\Delta\mathbf{h}_2$ in (52) can be formed as

$$\Delta\mathbf{h}_2 = \mathbf{B}_2\Delta\boldsymbol{\eta}_1 \tag{55}$$

where

$$\begin{aligned} [\mathbf{B}_2]_{1:3,1:3} &= \mathbf{I}_3 \\ [\mathbf{B}_2]_{1:3,1:3} &= 2diag(\dot{\mathbf{u}}) \\ [\mathbf{B}_2]_{1:3,4:6} &= 2diag(\mathbf{u}) \\ [\mathbf{B}_2]_{7,7} &= 1 \end{aligned} \tag{56}$$

The weighted least squares estimate of $\boldsymbol{\eta}_2^{\mathrm{o}}$ can be obtained from (52) as

$$\boldsymbol{\eta}_2 = (\mathbf{G}_2^T\mathbf{W}_2\mathbf{G}_2)^{-1}\mathbf{G}_2^T\mathbf{W}_2\mathbf{h}_2 \tag{57}$$

where $\mathbf{W}_2$ is the weighting matrix equal to

$$\begin{aligned} \mathbf{W}_2 &= \left[\mathrm{E}(\Delta\mathbf{h}_2\Delta\mathbf{h}_2^{\mathrm{T}})\right]^{-1} \\ &= \left[\mathbf{b}_2 cov(\boldsymbol{\eta}_1)\mathbf{b}_2^{\mathrm{T}}\right]^{-1} \end{aligned} \tag{58}$$

Using similar derivation, the covariance matrix of $\boldsymbol{\eta}_2$ can be written as

$$cov(\boldsymbol{\eta}_2) = (\mathbf{G}_2^{\mathrm{T}}\mathbf{W}_2\mathbf{G}_2)^{-1} \tag{59}$$

Finally, the refined estimate of source position and velocity can be acquired as

$$\begin{aligned} \mathbf{u} &= \boldsymbol{\eta}_2(1:3) \\ \dot{\mathbf{u}} &= \boldsymbol{\eta}_2(4:6)./\boldsymbol{\eta}_2(1:3) \end{aligned} \tag{60}$$

where the symbol "./" represents element by element division.

IV. CRLB AND THEORETICAL COVARIANCE

Theoretical analysis is performed in this section to prove the optimality properties of the proposed solution that the covariance matrix of the proposed solution is able to achieve the CRLB when some conditions are met.

A. CRAMÉR-RAO LOWER BOUND

For the source localization problem concerned in this paper, the unknowns including parameters of interest $\boldsymbol{\eta}^{\mathrm{o}} = [(\mathbf{u}^{\mathrm{o}})^{\mathrm{T}}, (\dot{u}^{\mathrm{o}})^{\mathrm{T}}]^{\mathrm{T}}$ and the nuisance parameters $\mathbf{n}^{\mathrm{o}} = [(\mathbf{r}^{\mathrm{o}})^{\mathrm{T}}, f_{\mathrm{c}}^{\mathrm{o}}]^{\mathrm{T}}$ are recast into a vector as $\boldsymbol{\phi}^{\mathrm{o}} = [(\boldsymbol{\eta}^{\mathrm{o}})^{\mathrm{T}}, (\mathbf{n}^{\mathrm{o}})^{\mathrm{T}}]^{\mathrm{T}}$, the observation vector including the AOA-FOA measurements $\mathbf{m}$, the receiver location parameters $\mathbf{r}$, and the carrier frequency f_{c}, are stacked into a vector $\mathbf{z} = [\mathbf{m}^{\mathrm{T}}, \mathbf{r}^{\mathrm{T}}, f_{\mathrm{c}}]^{\mathrm{T}} = [\mathbf{m}^{\mathrm{T}}, \mathbf{n}^{\mathrm{T}}]^{\mathrm{T}}$. Under the assumption that the AOA-FOA measurements, the receiver location parameters, and the carrier frequency, are independently Gaussian distributed, the logarithm of the probability density function (pdf) of $\mathbf{z}$ can be expressed as

$$\begin{aligned} \ln p(\mathbf{z}|\boldsymbol{\phi}^{\mathrm{o}}) &= \ln p(\mathbf{m}|\boldsymbol{\phi}^{\mathrm{o}}) + \ln p(\mathbf{n}|\boldsymbol{\phi}^{\mathrm{o}}) \\ &= \kappa - \frac{1}{2}(\mathbf{m} - \mathbf{m}^{\mathrm{o}})^{\mathrm{T}}\mathbf{Q}_{\mathbf{m}}^{-1}(\mathbf{m} - \mathbf{m}^{\mathrm{o}}) \\ &\quad - \frac{1}{2}(\mathbf{n} - \mathbf{n}^{\mathrm{o}})^{\mathrm{T}}\mathbf{Q}_{\mathbf{n}}^{-1}(\mathbf{n} - \mathbf{n}^{\mathrm{o}}) \end{aligned} \tag{61}$$

where κ is a constant. The CRLB for $\boldsymbol{\phi}^{\mathrm{o}}$ has the following expression

$$\mathrm{CRLB}(\boldsymbol{\phi}^{\mathrm{o}}) = -\mathrm{E}\left[\frac{\partial^2 \ln p(\mathbf{z}|\boldsymbol{\phi}^{\mathrm{o}})}{\partial\boldsymbol{\phi}^{\mathrm{o}}\partial\boldsymbol{\phi}^{\mathrm{o}\mathrm{T}}}\right]^{-1} \tag{62}$$

Combining (61) and the composition of the vectors $\mathbf{z}$ and $\boldsymbol{\phi}^{\mathrm{o}}$, we can rewrite (62) in submatrix form as

$$\mathrm{CRLB}(\boldsymbol{\phi}^{\mathrm{o}}) = \begin{bmatrix} \mathbf{X} & \mathbf{Y} \\ \mathbf{Y}^{\mathrm{T}} & \mathbf{z} \end{bmatrix} \tag{63}$$

where the submatrix $\mathbf{X}$, $\mathbf{Y}$ and $\mathbf{z}$ are given as

$$\mathbf{X} = -\mathrm{E}\left[\frac{\partial^2 \ln p(\mathbf{z}|\boldsymbol{\phi}^{\mathrm{o}})}{\partial \boldsymbol{\eta}^{\mathrm{o}} \partial \boldsymbol{\eta}^{\mathrm{oT}}}\right]^{-1} = \frac{\partial \mathbf{m}^{\mathrm{o}}}{\partial \boldsymbol{\eta}^{\mathrm{o}}} \mathbf{Q}_{\mathbf{m}}^{-1} \frac{\partial \mathbf{m}^{\mathrm{o}}}{\partial \boldsymbol{\eta}^{\mathrm{oT}}}$$
$$\mathbf{Y} = -\mathrm{E}\left[\frac{\partial^2 \ln p(\mathbf{z}|\boldsymbol{\phi}^{\mathrm{o}})}{\partial \boldsymbol{\eta}^{\mathrm{o}} \partial \mathbf{n}^{\mathrm{oT}}}\right]^{-1} = \frac{\partial \mathbf{m}^{\mathrm{o}}}{\partial \boldsymbol{\eta}^{\mathrm{o}}} \mathbf{Q}_{\mathbf{m}}^{-1} \frac{\partial \mathbf{m}^{\mathrm{o}}}{\partial \mathbf{n}^{\mathrm{oT}}}$$
$$\mathbf{Z} = -\mathrm{E}\left[\frac{\partial^2 \ln p(\mathbf{z}|\boldsymbol{\phi}^{\mathrm{o}})}{\partial \mathbf{n}^{\mathrm{o}} \partial \mathbf{n}^{\mathrm{oT}}}\right]^{-1} = \frac{\partial \mathbf{m}^{\mathrm{o}}}{\partial \mathbf{n}^{\mathrm{o}}} \mathbf{Q}_{\mathbf{m}}^{-1} \frac{\partial \mathbf{m}^{\mathrm{o}}}{\partial \mathbf{n}^{\mathrm{oT}}} + \mathbf{Q}_{\mathbf{n}}^{-1} \quad (64)$$

From (1), (2) and (5), the partial derivatives $\partial \mathbf{m}^{\mathrm{o}} / \partial \eta^{\mathrm{o}}$, $\partial \mathbf{m}^{\mathrm{o}} / \partial \mathbf{n}^{\mathrm{o}}$ can be detailed in (75)-(76) respectively.

The CRLB of η^{o} is the 6×6 upper-left block of CRLB($\boldsymbol{\phi}^{\mathrm{o}}$). Invoking the partitioned matrix inversion formula [32], we can rewrite CRLB($\boldsymbol{\eta}^{\mathrm{o}}$) as

$$\mathrm{CRLB}(\boldsymbol{\eta}^{\mathrm{o}}) = (\mathbf{X} - \mathbf{Y}\mathbf{z}^{-1}\mathbf{Y}^{\mathrm{T}})^{-1} \quad (65)$$

The trace of (65) is the minimum source position-velocity estimation RMSE of any unbiased estimator for the AOA-FOA based localization problem.

B. COVARIANCE MATRIX OF THE PROPOSED SOLUTION

Now, we deduce the estimation bias and covariance matrix of the proposed solution. By taking the differential of $\boldsymbol{\eta}_2^{\mathrm{o}}$ in (52), we can write the source position-velocity estimation error of the proposed solution as

$$\Delta\boldsymbol{\eta} = \begin{bmatrix} \Delta\mathbf{u} \\ \Delta\dot{\mathbf{u}} \end{bmatrix} = \mathbf{B}_3^{-1} \Delta\boldsymbol{\eta}_2 \quad (66)$$

where

$$\mathbf{B}_3 = \begin{bmatrix} \mathbf{I}_3 & O_3 \\ diag(\dot{\mathbf{u}}) & diag(\mathbf{u}) \end{bmatrix} \quad (67)$$

Taking the expectation of (66) yields $E(\Delta\boldsymbol{\eta}) \simeq 0_6$, indicating the proposed solution is unbiased given sufficiently small noises. Multiplying (66) by its transpose, and taking expectation, we get

$$cov(\boldsymbol{\eta}) = \mathbf{B}_3^{-1} cov(\eta_2) \mathbf{B}_3^{-\mathrm{T}} \quad (68)$$

We proceed to prove the equivalence between the CRLB in (65) and the covariance matrix in (68) given small noise conditions. For this purpose, Taking the inverse of (68), and substituting (59), (58), (47), (45) into (68) successively, leads to

$$cov(\boldsymbol{\eta})^{-1} = \mathbf{G}_3^T \mathbf{Q}_{\mathbf{m}}^{-1} \mathbf{G}_3 - \mathbf{G}_3^T \mathbf{Q}_{\mathbf{m}}^{-1} \mathbf{G}_4 (\mathbf{Q}_{\mathbf{n}}^{-1} + \mathbf{G}_4^T \mathbf{Q}_{\mathbf{m}}^{-1} \mathbf{G}_4)^{-1} \mathbf{G}_4^T \mathbf{Q}_{\mathbf{m}}^{-1} \mathbf{G}_3 \quad (69)$$

where

$$\mathbf{G}_3 = \mathbf{B}_1^{-1} \mathbf{G}_1 \mathbf{B}_2^{-1} \mathbf{G}_2 \mathbf{B}_3 \quad (70)$$
$$\mathbf{G}_4 = \mathbf{B}_1^{-1} \mathbf{D}_1 \quad (71)$$

Comparing (69) and (65) shows that they are identical in form. Further, when the AOA-FOA measurement noises, the carry frequency error, as well as the receiver location uncertainties are sufficiently small, direct evaluation reveals the following approximations

$$\frac{\partial \mathbf{m}^{\mathrm{o}}}{\partial \eta^{\mathrm{o}}} \simeq \mathbf{G}_3 \quad (72)$$
$$\frac{\partial \mathbf{m}^{\mathrm{o}}}{\partial \mathbf{n}^{\mathrm{o}}} \simeq \mathbf{G}_4 \quad (73)$$

Based on (72) and (73), we reach the conclusion that

$$cov(\boldsymbol{\eta}) \simeq CRLB(\boldsymbol{\eta}) \quad (74)$$

That is, the covariance matrix of the proposed solution attains the CRLB under the conditions of small AOA-FOA measurement noises, carry frequency error and receiver location uncertainties.

V. SIMULATION RESULTS

Monte Carlo simulations are performed in this section to evaluate the localization performance of proposed solution. In the simulation scenario, we consider an underwater acoustic application where the source emits a signal with carrier frequency $f_c^{\mathrm{o}} = 15$KHz and the signal propagation speed c is 1500 m/s. The source position is randomly generated from a 3-D space of $2 \times 2 \times 1$ km^3 centered at (0,0,500) m, the velocity is randomly generated from uniform distribution with the lower bound (-10,-10,-2) m/s and upper bound (10,10,2) m/s. The positions of the receivers are randomly generated from two regions with equal size of $2 \times 2 \times 0.1$km^3 centered at (0,0,50)m and (0,0,950)m, the velocity of the receivers are randomly generated from uniform distribution with the lower bound (-10,-10,-2)m/s and upper bound (10,10,2)m/s. The number of receivers M is 16 unless otherwise stated. The performance of the algorithms is assessed by the root mean square error (RMSE) of the source position and velocity estimate calculated from 100 randomly generated configurations, each with 100 ensemble runs. Note that the generated positions of the receivers must meet the condition that $\| \mathbf{s}_i^{\mathrm{o}} - \mathbf{s}_j^{\mathrm{o}} \| \geq$ 400m for $i, j = 1, 2, \ldots, M$ and $i < j$ to guarantee reasonable geometry. In each trial, the zero-mean Gaussian random noises with covariance/variance $\mathbf{Q}_{\mathrm{a}} = \sigma_{\mathrm{a}}^2 \mathbf{I}_{2M}$, $\mathbf{Q}_{\mathrm{f}} = \sigma_{\mathrm{f}}^2 \mathbf{I}_M$, $\mathbf{Q}_{\mathbf{r}} = \mathrm{blkdiag}(\sigma_{\mathrm{r}}^2 \mathbf{I}_{3M}, 0.01\sigma_{\mathrm{r}}^2 \mathbf{I}_{3M})$ and σ_{fc}^2 are added to the corresponding true values respectively. For comparison, the FOA-only localization algorithm proposed by M M Ahmed et al in [18] (designated as Ahmed's algorithm), and the AOA-FOA-based localization using Taylor-series method with the true source location as the initial guess (designated as Taylor-series method), the theoretical error, as well as the CRLB, are also investigated.

A. PERFORMANCE VERSUS AOA MEASUREMENT NOISE

We vary the AOA measurement noise level σ_{a} from 0.1° to 100°, while keeping the FOA measurement noise level $\sigma_{\mathrm{f}} = 10$Hz, the receiver location uncertainty level $\sigma_{\mathrm{r}} = 10$m, the carrier frequency error level $\sigma_{\mathrm{fc}} = 100$Hz. FIGURE 1 depicts the RMSEs of the proposed solution, the Taylor-series

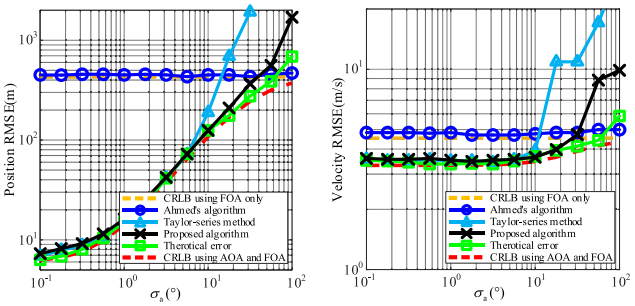

(a) Source position estimation (b) Source velocity estimation

FIGURE 1. Localization performance of the algorithms at different AOA measurement noise levels.

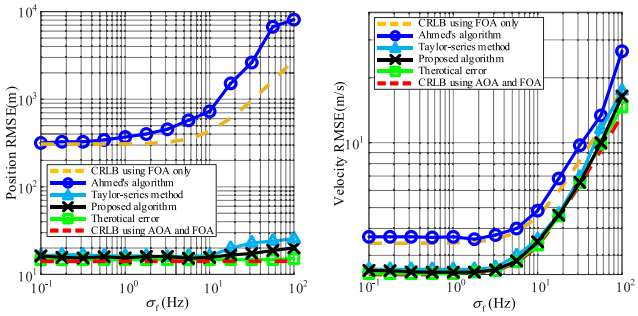

(a) Source position estimation (b) Source velocity estimation

FIGURE 2. Localization performance of the algorithms at different receiver location uncertainty levels.

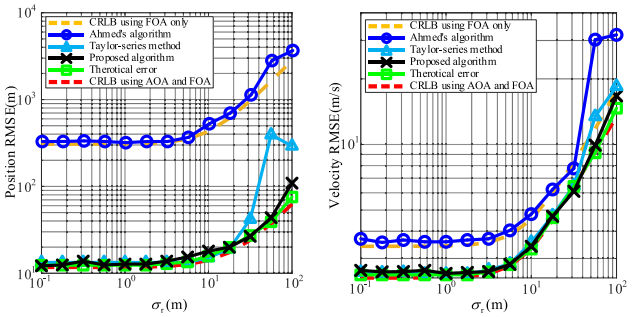

(a) Source position estimation (b) Source velocity estimation

FIGURE 3. Localization performance of the algorithms at different receiver location uncertainty levels.

method and Ahmed's algorithm at different AOA measurement noise levels. The proposed solution always achieves CRLB using AOA and FOA until the AOA measurement noise level increases to about 20°. This phenomenon, known as the ''threshold effect'' is caused by the second and higher error terms neglected in the linearization procedure of the measurement equations. The Taylor-series method deviates from the CRLB and gives an inaccurate estimate at about 5° that is 3 times lower than the proposed solution even though the true initial value is provided for the Taylor-series method. The reason lies in the local convergence or even divergence of the iteration. Compared with Ahmed's algorithm and the CRLB using FOA only, the proposed solution achieves significant improvement in localization accuracy at small AOA measurement noise levels, but as the AOA measurement noise increases, the gap between them decreases and gradually tends to zero. At the typical AOA measurement noise level of $\sigma_a = 1°$ which should not be hard to achieve, the proposed solution provides more than an order of magnitude increment in source position estimation accuracy, indicating the necessity of jointly using AOA measurements.

B. PERFORMANCE VERSUS FOA MEASUREMENT NOISE

The localization performance of the algorithms versus FOA measurement noise levels are evaluated in this part, where the FOA measurement noise level σ_f varies from 0.1Hz to 100Hz, and the AOA measurement noise level is set as $\sigma_a = 1°$, the receiver location uncertainty level $\sigma_r = 10$m, the carrier frequency error level $\sigma_{fc} = 100$Hz. The source position and velocity estimation RMSEs of the algorithms varying with FOA measurement noise level are shown in FIGURE 2.

One can see that the FOA measurement noise level has little effect on the source position estimation accuracy of the AOA-FOA localization. This is because the AOA measurement with noise level $\sigma_a = 1°$ dominates the estimation of source position. In contrast, the FOA only localization, in terms of both CRLB and RMSE, are significantly influenced by FOA measurement noises. Moreover, the proposed solution is very close to the CRLB using AOA and FOA at moderate measurement noise levels, and superior to the Taylor-series method at large FOA measurement noise levels. This indicates that the introduction of AOA measurements improves the localization robustness under different FOA measurement noises.

C. PERFORMANCE VERSUS RECEIVER LOCATION UNCERTAINTIES

Then we assess the performance of the algorithms at different receiver location uncertainty levels σ_r. The AOA and FOA measurement noise levels are set to be $\sigma_a = 1°$ and $\sigma_f = 10$Hz respectively, the carrier frequency error level is $\sigma_{fc} = 100$Hz. In FIGURE 3, we have plotted the position and velocity RMSEs of the algorithms as a function of the receiver location uncertainty level σ_r. As shown in the figure, the localization RMSEs of the algorithms are almost unchanged given sufficiently small receiver location uncertainties, but rises as the receiver location uncertainties increase over the region of moderate to large levels of receiver location uncertainties. The AOA-FOA localization including the proposed solution and Taylor-series method, outperforms the FOA-only localization, in terms of both CRLB and RMSE. Both the proposed solution and Taylor-series method show similar performance by achieving the CRLB over the region of small to moderate levels of receiver location uncertainties. But the proposed solution outperforms Taylor-series method by its ability to approach the CRLB at larger receiver location uncertainty level.

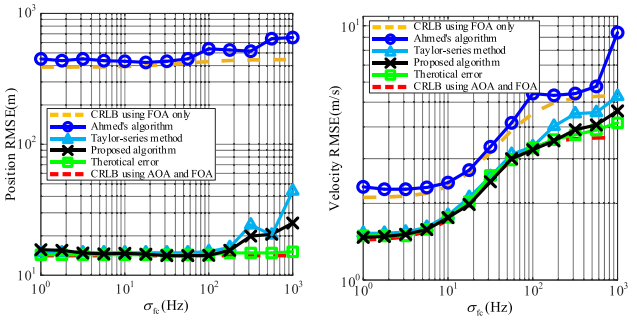

(a) Source position estimation (b) Source velocity estimation

FIGURE 4. Localization performance of the algorithms at different carrier frequency error levels.

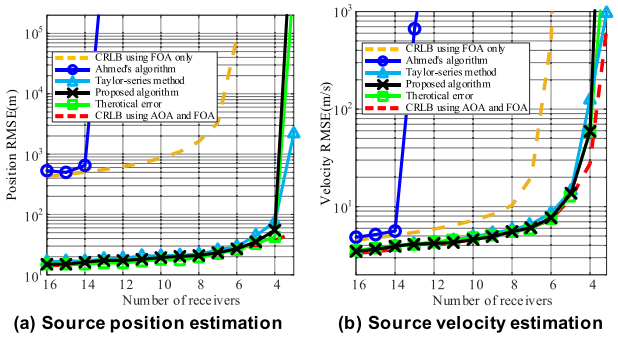

(a) Source position estimation (b) Source velocity estimation

FIGURE 5. Localization performance of the algorithms with different number of receivers.

D. PERFORMANCE VERSUS CARRIER FREQUENCY ERROR

In this scenario, we evaluate the performance of the algorithms at different carrier frequency error levels. FIGURE 4 presents the localization RMSEs of the algorithms as σ_{fc} increases while keeping $\sigma_{\text{a}} = 1°$, $\sigma_{\text{f}} = 10\text{Hz}$ and $\sigma_{\text{r}} = 10\text{m}$.

The source position estimation accuracy almost remains unchanged at different carrier frequency error levels, but the source velocity estimation accuracy is sensitive to the carrier frequency error levels. Both the proposed solution and Taylor-series method attain the CRLB over the region of small to moderate levels of carrier frequency error levels. They deviate from the CRLB at larger carrier frequency error levels, but the deviation of the proposed solution is significantly lower.

E. PERFORMANCE VERSUS RECEIVER NUMBER

In this scenario, we compare the performance of the algorithms when using different number of receivers for source localization. The other settings remain as $\sigma_{\text{a}} = 1°$, $\sigma_{\text{f}} = 10\text{Hz}$, $\sigma_{\text{r}} = 10\text{m}$ and $\sigma_{\text{fc}} = 100\text{Hz}$. FIGURE 5 presents the estimation performance of the algorithms with respect to the receiver number. For the localization scenario in FIGURE 5, Ahmed's algorithm requires at least 14 receivers to work properly due to the significant number of introduced auxiliary parameters and small number of measurements. By contrast, the proposed solution achieves the CRLB with only 4 receivers since we jointly using AOA and FOA measurements, and introduce only one auxiliary parameter. Taylor-series method requires only 3 receivers to operate since it does not introduce any auxiliary parameters, but it will be at the expense of local convergence and even divergence of the iteration.

F. GDOP ANALYSIS

To further explore the influence of different receiver configurations on the localization accuracy, we perform here the Geometric Dilution Of Precision (GDOP) analysis for source localization in FIGURE 6. The GDOP plot indicates the localization accuracy achievable with a particular geometry configuration of the receivers, where the color bar represents the normalized localization error. Lower values

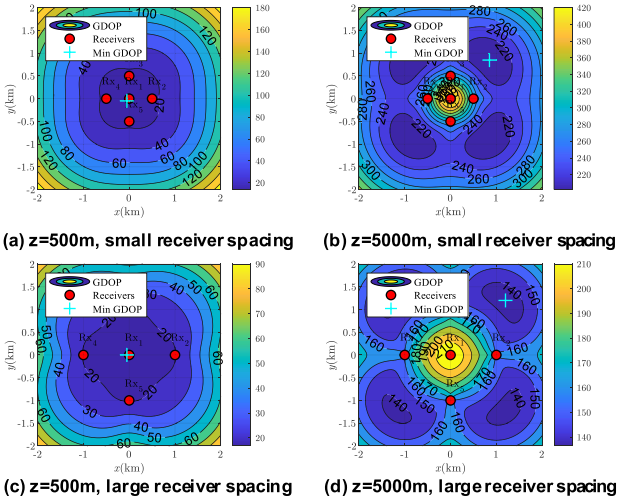

(a) z=500m, small receiver spacing (b) z=5000m, small receiver spacing

(c) z=500m, large receiver spacing (d) z=5000m, large receiver spacing

FIGURE 6. GDOP plots for different geometrical configurations.

indicate that the geometric configuration provides higher localization accuracy.

FIGURE 6 shows the GDOP contours for source localization by an array of receivers with large spacing and small spacing. By comparison, it can be found that, increasing the receiver spacing can improve the source localization accuracy. When the source height is low, the localization accuracy for the coverage area of the receivers is higher, and the highest localization accuracy is achieved at the center of the coverage area. The farther the source is from the center, the lower the localization accuracy is. But when the source height is too high, this law is no longer satisfied.

VI. CONCLUSION

In order to overcome the inherent defect of source localization using FOA measurements only, we address locating the moving source by jointly using AOA and FOA measurements. This paper designs a closed-form solution for AOA-FOA based source localization problem. This work borrows the basic idea of the well-known TSWLS by Chan and Ho, but is innovative for the AOA-FOA based source localization problem. The proposed solution can be divided into two stages. In the first stage, with the aid of the relationship between the source-receiver range and the AOA

measurement, the AOA-FOA measurement equations are linearized by introducing only one auxiliary parameter, and a rough estimate is obtained by using WLS minimization. In the second stage, the relation between the source location and the introduced auxiliary parameter is employed to refine the first stage estimate. By employing a joint localization scheme based on the AOA and FOA measurements, the proposed solution gives the source position and velocity estimate with much fewer receivers and nuisance parameters in comparison with the state-of-the-art FOA-only localization method. Due to the application of TSWLS framework in this algorithm, there is no convergence or initialization problem, as in iterative method. Theoretical analysis and numerical simulations are performed, verifying the proposed solution achieves the CRLB under small Gaussian noise conditions and outperforms the FOA-only method in terms of CRLB and RMSE.

APPENDIX A
EVALUATION OF THE PARTIAL DERIVATIVES

According to the AOA and FOA equations in (1), (2) and (5), the partial derivatives of m^{o} with respect to the unknown parameters $\boldsymbol{\eta}^{\mathrm{o}}$ and $\mathbf{n}^{\mathrm{o}}$ are respectively given by

$$
\begin{aligned}
&\left[\frac{\partial \mathbf{m}^{\mathrm{o}}}{\partial \eta^{\mathrm{o}}}\right]_{m,1} \\
&= -\frac{(y^{\mathrm{o}} - y_m^{\mathrm{o}})}{(x^{\mathrm{o}} - x_m^{\mathrm{o}})^2 + (y^{\mathrm{o}} - y_m^{\mathrm{o}})^2} \\
&\left[\frac{\partial \mathbf{m}^{\mathrm{o}}}{\partial \eta^{\mathrm{o}}}\right]_{m,2} \\
&= \frac{(x^{\mathrm{o}} - x_m^{\mathrm{o}})}{(x^{\mathrm{o}} - x_m^{\mathrm{o}})^2 + (y^{\mathrm{o}} - y_m^{\mathrm{o}})^2} \\
&\left[\frac{\partial \mathbf{m}^{\mathrm{o}}}{\partial \eta^{\mathrm{o}}}\right]_{M+m,1} \\
&= \frac{-(x^{\mathrm{o}} - x_m^{\mathrm{o}})(z^{\mathrm{o}} - z_m^{\mathrm{o}})}{\| \mathbf{u}^{\mathrm{o}} - \mathbf{s}_m^{\mathrm{o}} \|^2 \sqrt{(x^{\mathrm{o}} - x_m^{\mathrm{o}})^2 + (y^{\mathrm{o}} - y_m^{\mathrm{o}})^2}} \\
&\left[\frac{\partial \mathbf{m}^{\mathrm{o}}}{\partial \eta^{\mathrm{o}}}\right]_{M+m,2} \\
&= \frac{-(y^{\mathrm{o}} - y_m^{\mathrm{o}})(z^{\mathrm{o}} - z_m^{\mathrm{o}})}{\| \mathbf{u}^{\mathrm{o}} - \mathbf{s}_m^{\mathrm{o}} \|^2 \sqrt{(x^{\mathrm{o}} - x_m^{\mathrm{o}})^2 + (y^{\mathrm{o}} - y_m^{\mathrm{o}})^2}} \\
&\left[\frac{\partial \mathbf{m}^{\mathrm{o}}}{\partial \eta^{\mathrm{o}}}\right]_{M+m,3} \\
&= \frac{\sqrt{(x^{\mathrm{o}} - x_m^{\mathrm{o}})^2 + (y^{\mathrm{o}} - y_m^{\mathrm{o}})^2}}{\| \mathbf{u}^{\mathrm{o}} - \mathbf{s}_m^{\mathrm{o}} \|^2} \\
&\left[\frac{\partial \mathbf{m}^{\mathrm{o}}}{\partial \eta^{\mathrm{o}}}\right]_{2M+m,1:3} \\
&= -\frac{f_{\mathrm{c}}^{\mathrm{o}}}{c}\left(\frac{(\dot{\mathbf{u}}^{\mathrm{o}} - \dot{\mathbf{s}}_m^{\mathrm{o}})^T}{\| \mathbf{u}^{\mathrm{o}} - \mathbf{s}_m^{\mathrm{o}} \|} - \frac{(\mathbf{u}^{\mathrm{o}} - \mathbf{s}_m^{\mathrm{o}})^T (\dot{\mathbf{u}}^{\mathrm{o}} - \dot{\mathbf{s}}_m^{\mathrm{o}})(\mathbf{u}^{\mathrm{o}} - \mathbf{s}_m^{\mathrm{o}})^T}{\| \mathbf{u}^{\mathrm{o}} - \mathbf{s}_m^{\mathrm{o}} \|^3}\right) \\
&\left[\frac{\partial \mathbf{m}^{\mathrm{o}}}{\partial \eta^{\mathrm{o}}}\right]_{2M+m,4:6} \\
&= -\frac{f_{\mathrm{c}}^{\mathrm{o}}}{c}\frac{(\mathbf{u}^{\mathrm{o}} - \mathbf{s}_m^{\mathrm{o}})^{\mathrm{T}}}{\| \mathbf{u}^{\mathrm{o}} - \mathbf{s}_m^{\mathrm{o}} \|}
\end{aligned} \tag{75}
$$

$$
\begin{aligned}
&\left[\frac{\partial \mathbf{m}^{\mathrm{o}}}{\partial \mathbf{n}^{\mathrm{o}}}\right]_{m,3m-2} \\
&= \frac{(y^{\mathrm{o}} - y_m^{\mathrm{o}})}{(x^{\mathrm{o}} - x_m^{\mathrm{o}})^2 + (y^{\mathrm{o}} - y_m^{\mathrm{o}})^2} \\
&\left[\frac{\partial \mathbf{m}^{\mathrm{o}}}{\partial \mathbf{n}^{\mathrm{o}}}\right]_{m,3m-1} \\
&= \frac{-(x^{\mathrm{o}} - x_m^{\mathrm{o}})}{(x^{\mathrm{o}} - x_m^{\mathrm{o}})^2 + (y^{\mathrm{o}} - y_m^{\mathrm{o}})^2} \\
&\left[\frac{\partial \mathbf{m}^{\mathrm{o}}}{\partial \mathbf{n}^{\mathrm{o}}}\right]_{M+m,3m-2} \\
&= \frac{(x^{\mathrm{o}} - x_m^{\mathrm{o}})(z^{\mathrm{o}} - z_m^{\mathrm{o}})}{\| \mathbf{u}^{\mathrm{o}} - \mathbf{s}_m^{\mathrm{o}} \|^2 \sqrt{(x^{\mathrm{o}} - x_m^{\mathrm{o}})^2 + (y^{\mathrm{o}} - y_m^{\mathrm{o}})^2}} \\
&\left[\frac{\partial \mathbf{m}^{\mathrm{o}}}{\partial \mathbf{n}^{\mathrm{o}}}\right]_{M+m,3m-1} \\
&= \frac{(y^{\mathrm{o}} - y_m^{\mathrm{o}})(z^{\mathrm{o}} - z_m^{\mathrm{o}})}{\| \mathbf{u}^{\mathrm{o}} - \mathbf{s}_m^{\mathrm{o}} \|^2 \sqrt{(x^{\mathrm{o}} - x_m^{\mathrm{o}})^2 + (y^{\mathrm{o}} - y_m^{\mathrm{o}})^2}} \\
&\left[\frac{\partial \mathbf{m}^{\mathrm{o}}}{\partial \mathbf{n}^{\mathrm{o}}}\right]_{M+m,3m} \\
&= -\frac{\sqrt{(x^{\mathrm{o}} - x_m^{\mathrm{o}})^2 + (y^{\mathrm{o}} - y_m^{\mathrm{o}})^2}}{\| \mathbf{u}^{\mathrm{o}} - \mathbf{s}_m^{\mathrm{o}} \|^2} \\
&\left[\frac{\partial \mathbf{m}^{\mathrm{o}}}{\partial \mathbf{n}^{\mathrm{o}}}\right]_{2M+m,3m-2:3m} \\
&= \frac{f_{\mathrm{c}}^{\mathrm{o}}}{c}\left(\frac{(\dot{\mathbf{u}}^{\mathrm{o}} - \dot{\mathbf{s}}_m^{\mathrm{o}})^T}{\| \mathbf{u}^{\mathrm{o}} - \mathbf{s}_m^{\mathrm{o}} \|} - \frac{(\mathbf{u}^{\mathrm{o}} - \mathbf{s}_m^{\mathrm{o}})^T (\dot{\mathbf{u}}^{\mathrm{o}} - \dot{\mathbf{s}}_m^{\mathrm{o}})(\mathbf{u}^{\mathrm{o}} - \mathbf{s}_m^{\mathrm{o}})^T}{\| \mathbf{u}^{\mathrm{o}} - \mathbf{s}_m^{\mathrm{o}} \|^3}\right) \\
&\left[\frac{\partial \mathbf{m}^{\mathrm{o}}}{\partial \mathbf{n}^{\mathrm{o}}}\right]_{2M+m,3M+3m-2:3M+3m} \\
&= \frac{f_{\mathrm{c}}^{\mathrm{o}}}{c}\frac{(\mathbf{u}^{\mathrm{o}} - \mathbf{s}_m^{\mathrm{o}})^{\mathrm{T}}}{\| \mathbf{u}^{\mathrm{o}} - \mathbf{s}_m^{\mathrm{o}} \|} \\
&\left[\frac{\partial \mathbf{m}^{\mathrm{o}}}{\partial \mathbf{n}^{\mathrm{o}}}\right]_{2M+m,6M+1} \\
&= 1 - \frac{(\mathbf{u}^{\mathrm{o}} - \mathbf{s}_m^{\mathrm{o}})^{\mathrm{T}} (\dot{\mathbf{u}}^{\mathrm{o}} - \dot{\mathbf{s}}_m^{\mathrm{o}})}{c \| \mathbf{u}^{\mathrm{o}} - \mathbf{s}_m^{\mathrm{o}} \|}
\end{aligned} \tag{76}
$$

for $m = 1, 2, \ldots, M$ and zeros elsewhere.

REFERENCES

[1] J. Zhang and P. Wu, "Joint sampling synchronization and source localization for wireless acoustic sensor networks," *IEEE Commun. Lett.*, vol. 24, no. 5, pp. 1020–1023, May 2020.

[2] K. Li, Y. Jiao, Y. Song, J. Li, and C. Yue, "Passive localization of multiple sources using joint RSS and AOA measurements in spectrum sharing system," *China Commun.*, vol. 18, no. 12, pp. 65–80, Dec. 2021.

[3] S. K. Yadav and N. V. George, "Coarray MUSIC-group delay: High-resolution source localization using non-uniform arrays," *IEEE Trans. Veh. Technol.*, vol. 70, no. 9, pp. 9597–9601, Sep. 2021.

[4] M. Alves, R. Coelho, and E. Dranka, "Effective acoustic energy sensing exploitation for target sources localization in urban acoustic scenes," *IEEE Sensors Lett.*, vol. 4, no. 2, pp. 1–4, Feb. 2020.

[5] M. Pauley and J. H. Manton, "The existence question for maximum-likelihood estimators in time-of-arrival-based localization," *IEEE Signal Process. Lett.*, vol. 25, no. 9, pp. 1354–1358, Sep. 2018.

[6] S. Wu, S. Zhang, and D. Huang, "A TOA-based localization algorithm with simultaneous NLOS mitigation and synchronization error elimination," *IEEE Sensors Lett.*, vol. 3, no. 3, pp. 1–4, Mar. 2019.

[7] Z. Zhang, Q. Chang, N. Zhao, and H. Wang, "TOA-based relative localization with reflecting signal paths assisted: Algorithm and performance analysis," *IEEE Sensors Lett.*, vol. 6, no. 9, pp. 1–4, Sep. 2022.
[8] Y. T. Chan, H. Y. C. Hang, and P.-C. Ching, "Exact and approximate maximum likelihood localization algorithms," *IEEE Trans. Veh. Technol.*, vol. 55, no. 1, pp. 10–16, Jan. 2006.
[9] Y. Zou and H. Liu, "TDOA localization with unknown signal propagation speed and sensor position errors," *IEEE Commun. Lett.*, vol. 24, no. 5, pp. 1024–1027, May 2020.
[10] Y. Zou and H. Liu, "Semidefinite programming methods for alleviating clock synchronization bias and sensor position errors in TDOA localization," *IEEE Signal Process. Lett.*, vol. 27, pp. 241–245, 2020.
[11] X. Ma, T. Ballal, H. Chen, O. Aldayel, and T. Y. Al-Naffouri, "A maximum-likelihood TDOA localization algorithm using Difference-of-Convex programming," *IEEE Signal Process. Lett.*, vol. 28, pp. 309–313, 2021.
[12] Z. Gong, C. Li, F. Jiang, and J. Zheng, "AUV-aided localization of underwater acoustic devices based on Doppler shift measurements," *IEEE Trans. Wireless Commun.*, vol. 19, no. 4, pp. 2226–2239, Apr. 2020.
[13] A. Amar and A. J. Weiss, "Localization of narrowband radio emitters based on Doppler frequency shifts," *IEEE Trans. Signal Process.*, vol. 56, no. 11, pp. 5500–5508, Nov. 2008.
[14] T. Tirer and A. J. Weiss, "High resolution localization of narrowband radio emitters based on Doppler frequency shifts," *Signal Process.*, vol. 141, pp. 288–298, Dec. 2017.
[15] N. H. Nguyen and K. Doğançay, "Closed-form algebraic solutions for 3-D Doppler-only source localization," *IEEE Trans. Wireless Commun.*, vol. 17, no. 10, pp. 6822–6836, Oct. 2018.
[16] L. Deng, P. Wei, Z. Zhang, and H. Zhang, "Doppler frequency shift based source localization in presence of sensor location errors," *IEEE Access*, vol. 6, pp. 59752–59760, 2018.
[17] M. M. Ahmed, K. C. Ho, and G. Wang, "Localization of a moving source by frequency measurements," *IEEE Trans. Signal Process.*, vol. 68, pp. 4839–4854, 2020.
[18] M. M. Ahmed, K. C. Ho, and G. Wang, "3-D target localization and motion analysis based on Doppler shifted frequencies," *IEEE Trans. Aerosp. Electron. Syst.*, vol. 58, no. 2, pp. 815–833, Apr. 2022.
[19] J. Li, F. Guo, and W. Jiang, "A linear-correction least-squares approach for geolocation using FDOA measurements only," *Chin. J. Aeronaut.*, vol. 25, no. 5, pp. 709–714, Oct. 2012.
[20] K. C. Pine, S. Pine, and M. Cheney, "The geometry of far-field passive source localization with TDOA and FDOA," *IEEE Trans. Aerosp. Electron. Syst.*, vol. 57, no. 6, pp. 3782–3790, Dec. 2021.
[21] Y. Pei, X. Li, L. Yang, and F. Guo, "A closed-form solution for source localization using FDOA measurements only," *IEEE Commun. Lett.*, vol. 27, no. 1, pp. 115–119, Jan. 2023.
[22] Q. Yan and J. Chen, "Robust AOA-based source localization in correlated measurement noise via nonconvex sparse optimization," *IEEE Commun. Lett.*, vol. 25, no. 5, pp. 1529–1533, May 2021.
[23] T.-K. Le and K. C. Ho, "Joint source and sensor localization by angles of arrival," *IEEE Trans. Signal Process.*, vol. 68, pp. 6521–6534, 2020.
[24] L. Kraljevic, M. Russo, M. Stella, and M. Sikora, "Free-field TDOA-AOA sound source localization using three soundfield microphones," *IEEE Access*, vol. 8, pp. 87749–87761, 2020.
[25] Y. Xue, W. Su, H. Wang, D. Yang, and J. Ma, "A model on indoor localization system based on the time difference without synchronization," *IEEE Access*, vol. 6, pp. 34179–34189, 2018.
[26] A. Catovic and Z. Sahinoglu, "The Cramer–Rao bounds of hybrid TOA/RSS and TDOA/RSS location estimation schemes," *IEEE Commun. Lett.*, vol. 8, no. 10, pp. 626–628, Oct. 2004.
[27] K. C. Ho and Y. T. Chan, "An asymptotically unbiased estimator for bearings-only and Doppler-bearing target motion analysis," *IEEE Trans. Signal Process.*, vol. 54, no. 3, pp. 809–822, Mar. 2006.
[28] M. Shasha and S. Ning, "An iterative extended Kalman filter algorithm applying Doppler and bearing measurements for underwater passive target tracking," in *Proc. IEEE Int. Conf. Inf. Technol., Big Data Artif. Intell. (ICIBA)*, vol. 1, Nov. 2020, pp. 1318–1322.
[29] Y. T. Chan and S. W. Rudnicki, "Bearings-only and Doppler-bearing tracking using instrumental variables," *IEEE Trans. Aerosp. Electron. Syst.*, vol. 28, no. 4, pp. 1076–1083, Oct. 1992.
[30] L. Yang, M. Sun, and K. C. Ho, "Doppler-bearing tracking in the presence of observer location error," *IEEE Trans. Signal Process.*, vol. 56, no. 8, pp. 4082–4087, Aug. 2008.
[31] K. C. Ho and W. Xu, "An accurate algebraic solution for moving source location using TDOA and FDOA measurements," *IEEE Trans. Signal Process.*, vol. 52, no. 9, pp. 2453–2463, Sep. 2004.
[32] S. M. Kay, *Fundamentals of Statistical Signal Processing: Estimation Theory*. Englewood Cliffs, NJ, USA: Prentice-Hall, 1993.

ZHU JIANDONG received the M.S. degree from the Zhengzhou Information Technology Institute, Zhengzhou, China, in 2006, and the Ph.D. degree from the National Digital Switching System Engineering Technology Center, Zhengzhou, in 2013. From 2014 to 2020, he was an Associate Research Fellow with the State Key Laboratory of Complex Electromagnetic Environment Effects on Electronics and Information System (CEMEE), Luoyang, China. His current research interests include radar signal processing, passive location, and C-UAS.

DING TING received the M.S. degree from Northwestern Polytechnical University, in 2008, and the Ph.D. degree from the National Digital Switching System Engineering Technology Center, in 2019. She is currently a Senior Engineer with the Henan High-Speed Railway Operation and Technological Research Center, Zhengzhou, China. Her current research interests include mmWave massive MIMO, hybrid precoding, and channel estimation.

QIAO LIJUAN received the bachelor's degree in electronic information engineering and the master's degree in electronic and communication engineering from the National Digital Switching System Engineering Technology Center, in 2013 and 2016, respectively. She mainly involved in the field of electronic information and information security.